In: Solution Chemistry
Editor: Yongliang Xiong
ISBN: 978-1-53613-101-7
© 2018 Nova Science Publishers, Inc.

No part of this digital document may be reproduced, stored in a retrieval system or transmitted commercially in any form or by any means. The publisher has taken reasonable care in the preparation of this digital document, but makes no expressed or implied warranty of any kind and assumes no responsibility for any errors or omissions. No liability is assumed for incidental or consequential damages in connection with or arising out of information contained herein. This digital document is sold with the clear understanding that the publisher is not engaged in rendering legal, medical or any other professional services.

Chapter 2

EXPERIMENTAL DETERMINATION OF BRUCITE SOLUBILITY IN NACL SOLUTIONS AT ELEVATED TEMPERATURES

Leslie Kirkes and Yongliang Xiong*
Sandia National Laboratories (SNL), Carlsbad, NM, US

ABSTRACT

Salt formations have been recommended for nuclear waste isolation since the 1950's by the U.S. National Academy of Science. This recommendation has been implemented in southeast New Mexico where the Waste Isolation Pilot Plant (WIPP) has been built to isolate defense-related transuranic waste. The WIPP is located in a bedded salt formation, the Salado Formation. Placement of crystalline MgO, which hydrates rapidly to form brucite, is the only engineered barrier employed in the WIPP design. The MgO acts as a chemical conditioner in the WIPP repository in controlling the fugacity of carbon dioxide. Similarly, an $Mg(OH)_2$-based engineered barrier is proposed for the German Asse salt mine repository. Thus, the solubility of brucite is of interest to salt repository programs which can expect a variety of temperatures within

* Corresponding Author Email: yxiong@sandia.gov.

the repository and a variety of fluids (brines) coming in contact with the waste.

Salt repository programs are not the only programs that stand to benefit from the information presented in this book chapter. There are other applications where this information is of interest. In natural environments brucite frequently precipitates from hyperalkaline hydrothermal fluids with high ionic strengths. For instance, brucite chimneys have been observed to form at elevated temperatures in ocean floors. The information presented in this work can be used to accurately model the formation of such brucite chimneys.

In this study, we have determined solubilities of brucite as a function of ionic strength in NaCl solutions to I = 5.6 mol•kg^{-1} at elevated temperatures to 353.15 K. In our solubility measurements, we first independently determined the correction factors for converting pH readings to pH_m (negative logarithm of hydrogen ion concentration on a molal scale, mol•kg^{-1}) in NaCl solutions from 0.01 to 5.6 mol•kg^{-1} at elevated temperatures. Using the SIT model, we obtain the solubility constants for brucite at infinite dilution as a function of temperature,

$$Mg(OH)_2(cr) + 2H^+ \rightleftharpoons Mg^{2+} + 2H_2O(l)$$

which can be described by the following expression,

$$\log_{10} K^0_{s2} = \frac{4306.8369}{T} + 2.6383$$

where T is temperature in K. This expression can be used from 273.15 K to 373.15 K.

Keywords: nuclear waste management, hydrolysis, Specific Ion Interaction Theory (SIT), Salt Formations, High Level Nuclear Waste, Waste Isolation Pilot Plant (WIPP), Brucite chimneys

INTRODUCTION

Salt formations are ideal for nuclear waste isolation, as noted by the National Academy of Science as early as the 1950's (U.S. National Academy of Science, 1957). There are already two repositories in salt formations in the world. The Waste Isolation Pilot Plant (WIPP) is a U.S.

Department of Energy (DOE) repository for disposal of defense transuranic waste. The WIPP is located in a bedded salt formation and is located in southeast New Mexico, USA. The German Asse repository is located in a domal salt formation (Schűessler et al., 2001).

In WIPP and Asse, brucite, a hydrated magnesium oxide mineral, influences the near-field geochemistry. This is because the WIPP will use crystalline MgO and Asse will use hydrated MgO emplaced alongside the waste as an engineered barrier (e.g., Krumhansl et al., 2000; Xiong and Snider, 2008). MgO has been placed in the WIPP since operations began. An $Mg(OH)_2$-based engineered barrier is also proposed for the German Asse salt mine repository (Schűessler et al., 2001). Crystalline MgO hydrates rapidly forming brucite, which based on its solubility, conditions the near-field environment and controls the fugacity of carbon dioxide. Therefore, brucite solubilities in high ionic strength solutions at various temperatures are required to predict the near-field geochemical environment both for WIPP and Asse. Of note is that the German Asse repository is expected to witness elevated temperatures and both repositories have high ionic strength brines present.

In addition, there are several candidate repositories in salt formations, including Gorleben (Schwartz, 2012), Morsleben (Behlau and Mingerzahn, 2001; Brewitz et al., 2008) in Germany, and the sites in the Mid North Sea High and the East Midlands Shelf in UK (Stewart, 2002). Although the engineered barrier for those candidate repositories has not been decided, MgO- or $Mg(OH)_2$-based engineered barrier would be a strong candidate.

The solubility of brucite as a function of ionic strength at room temperature has been well characterized (e.g., Altmaier et al., 2003; Xiong, 2003, 2008). However, the solubilities of brucite at elevated temperatures in high ionic strength solutions, which may be relevant to disposal of heat-generating waste in salt formations is not well known.

In addition, brucite has been observed to form in saline, hyperalkaline, hydrothermal fluids (Monnin et al., 2014; Okumura et al., 2016). In these environments, the temperatures are elevated up to 90ºC, and the fluids are of high ionic strength, and brucite supports unique ecosystems with dense *Phyllochaetopterus* (e.g., Okumura et al., 2016). Therefore, brucite

solubilities at elevated temperatures in high ionic strength solutions contribute to modeling the formation of brucite in those environments.

The objective of this work is to experimentally determine solubilities of brucite as a function of ionic strength in NaCl solutions up to 5.6 mol•kg^{-1} at elevated temperatures. In our work, the correction factors that are used to convert pH readings to pcH (negative logarithm of hydrogen ion concentration on a molar scale) are separately determined.

METHODS

All materials (e.g., NaCl, $Mg(OH)_2$) used in this study are reagent grade from Fisher Scientific. Deionized (DI) water with 18.3 MΩ was produced by a *PURELAB Classic Water System* from ELGA. Degassed DI water was used for preparation of all starting solutions. The degassed DI water was obtained by bubbling high purity argon gas (purity 99.996%) from Matheson Tri-Gas, Inc., through DI water for at least one hour, following a procedure similar to that described by Wood et al., (2002). Starting solutions were prepared such that the equilibrium solubility was approached from undersaturation with respect to brucite. The starting solutions included NaCl solutions ranging from 0.010 to 5.6 mol•kg^{-1} NaCl.

The experiments were conducted at five temperatures from 40 ± 0.05ºC through 80 ± 0.05ºC at an increment of 10ºC. For each of the experiments undersaturated with respect to brucite, about 1 gram of $Mg(OH)_2$ (cr) was placed into a 150 mL high density polyethylene plastic bottle containing 100 mL of starting solution.

At specific intervals, the pH reading of each experimental solution was measured with an Orion-Ross combination pH glass electrode. Before each measurement, the pH meter was calibrated with three pH buffers (pH 4, pH 7 and pH 10) at the experimental temperature. For solutions with ionic strengths higher than 0.10 mol•kg^{-1}, the observed solution pH readings were converted to negative logarithm of hydrogen-ion concentrations (pcH) on a molar scale using a correction factor, *A* (see below).

The relation between the pH electrode reading (pH_{ob}) and pcH can be expressed as (Xiong et al., 2010):

$$pcH = pH_{ob} + A_M \quad (1)$$

where A_M is a correction factor on a molar scale. The correction factors were determined at the experimental temperatures as a function of ionic strength by following a procedure similar to that of Xiong et al., (2010). Then, pcH's were converted to negative logarithms of hydrogen-ion concentrations (pH_m) on a molal scale according to the following equation (Xiong et al., 2010),

$$pH_m = pH_{ob} + A_m = pH_{ob} + A_M - \log \Theta \quad (2)$$

where A_m is a correction factor on a molal scale, and Θ is a conversion factor from molality to molarity, which is computed from the density of a NaCl solution at the concentration and temperature of interest from Sőhnel and Novotný (1985).

After a pH measurement was taken, certain amounts of solution were withdrawn from an experimental run. The solution was filtered using a 0.2 μm syringe filter. The filtered solution was then weighed and acidified with 0.5 mL of concentrated HNO_3 (TraceMetal grade from Fisher Scientific). The extracted solution was then diluted to 10 mL with DI water so that dissolved ΣMg^{2+} and Na^+ concentrations could be determined.

Elemental concentrations of magnesium were determined by using the Perkin Elmer Optima 8300 inductively coupled plasma atomic emission spectrometer (ICP-AES). Calibration blanks and standards were precisely matched with experimental matrices. The correlation coefficients of calibration curves in all measurements were better than 0.9995. The analytical precision is better than 1.00% in terms of the relative standard deviation (RSD) based on replicate analyses.

Solid phase identification was performed by using a Bruker AXS, Inc., D8 Advance X-ray diffractometer (XRD) with a Sol-X detector. XRD

patterns were collected using CuKα radiation at a scanning rate of 1.33°/min for a 2θ range of 10–90°. There is no new phase observed.

Scanning electron microscope (SEM) analyses of the starting material, $Mg(OH)_2$(cr), indicate that the majority of particles are larger than 1 μm (Figure 1). The particle size of the solubility-controlling phase, brucite, after the experiments, is similar to that of the starting material (Figures 2 and 3). The particle size of brucite in the experiments performed in this work is similar to that observed in Xiong (2008). Accordingly, based on the assessment in Xiong (2008), the surface energy contribution to the solubility of brucite is insignificant in this study.

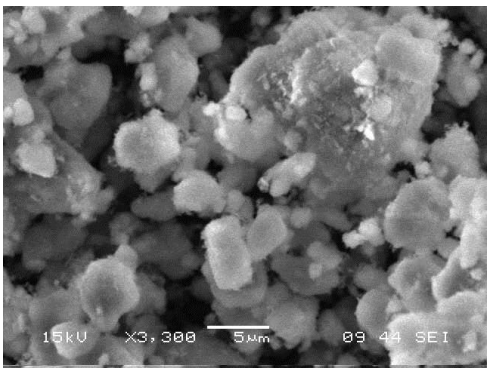

Figure 1. Scanning electron microscope (SEM) image of the starting material, $Mg(OH)_2$(cr).

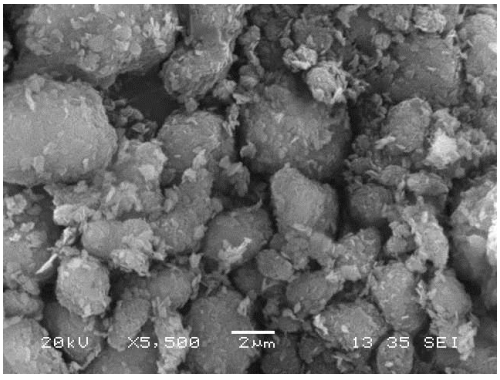

Figure 2. Scanning electron microscope (SEM) image of brucite, $Mg(OH)_2$(cr), in 1.0 mol•kg^{-1} NaCl solution at 80°C, after the experiment.

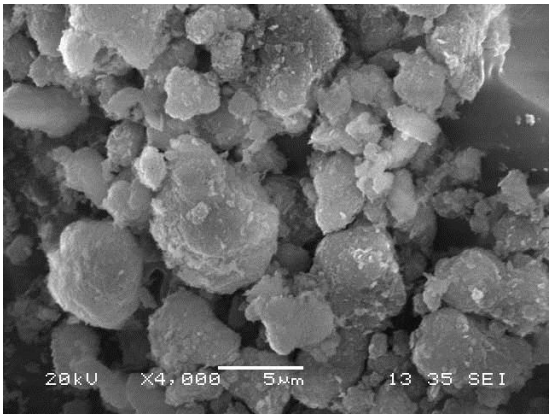

Figure 3. Scanning electron microscope (SEM) image of brucite, $Mg(OH)_2$(cr), in 5.6 mol•kg^{-1} NaCl solution at 80°C, after the experiment.

EXPERIMENTAL RESULTS AND THERMODYNAMIC CALCULATIONS

Correction Factors at Elevated Temperatures as a Function of Ionic Strength

In Table 1, the experimentally determined correction factors in NaCl solutions at various temperatures as a function of ionic strength are listed. In addition, the correlations between correction factors and molalities of NaCl are presented as linear equations at each temperature in Table 2, based on the experimental data from Table 1.

Solubility of Brucite in NaCl Solutions at Elevated Temperatures

In Table 3, the raw experimental data from this study are tabulated. The total magnesium concentrations are the result of the following reactions:

$$Mg(OH)_2(cr) + 2H^+ \rightleftharpoons Mg^{2+} + 2H_2O(l) \quad (3)$$

$$Mg^{2+} + H_2O(l) \rightleftharpoons MgOH^+ + H^+ \quad (4)$$

Table 1. Experimentally determined correction factors at different temperatures as a function of ionic strength

Temperature, ºC	**NaCl, mol•kg^{-1}**	**A_M**	**A_m**
40	1.0	0.007	–0.00469
	2.1	0.191	0.170
	3.2	0.363	0.332
	4.4	0.564	0.522
	5.6	0.762	0.708
50	1.0	–0.01	–0.0237
	2.1	0.237	0.214
	3.2	0.372	0.338
	4.4	0.579	0.535
	5.6	0.750	0.695
60	1.0	0.08	0.0641
	2.1	0.218	0.192
	3.2	0.433	0.398
	4.4	0.637	0.590
	5.6	0.758	0.700
70	1.0	0.121	0.105
	2.1	0.238	0.212
	3.2	0.429	0.394
	4.4	0.597	0.550
	5.6	0.770	0.712
80	1.0	0.124	0.103
	2.1	0.251	0.221
	3.2	0.457	0.417
	4.4	0.615	0.564
	5.6	0.713	0.651

Table 2. Concentration dependence of correction factors at constant temperatures

T, °C	A_M as a function of molality	A_m as a function of molality
40	$A_M = -0.1565 + 0.1638\ m_{NaCl}$	$A_m = -0.1587 + 0.1547\ m_{NaCl}$
50	$A_M = -0.1417 + 0.1618\ m_{NaCl}$	$A_m = -0.1462 + 0.1527\ m_{NaCl}$
60	$A_M = -0.07746 + 0.1542\ m_{NaCl}$	$A_m = -0.08406 + 0.1451\ m_{NaCl}$
70	$A_M = -0.03886 + 0.1441\ m_{NaCl}$	$A_m = -0.04546 + 0.1351\ m_{NaCl}$
80	$A_M = -0.004252 + 0.1338\ m_{NaCl}$	$A_m = -0.01614 + 0.1249\ m_{NaCl}$

In this work, we compute the equilibrium quotients for Reaction (3), Q_{s2}, based on our solubility data. The free magnesium concentrations, $m_{Mg^{2+}}$, are calculated from total magnesium concentrations after correcting contributions from $MgOH^+$, m_{MgOH^+}, according to the equilibrium quotients for Reaction (4), $Q_{1,1}$, from Palmer and Wesolowski (1997) in NaCl solutions at the respective temperatures and ionic strengths:

$$m_{\Sigma Mg} = m_{Mg^{2+}} + m_{MgOH^+} \tag{5}$$

$$Q_{1,1} = \frac{m_{MgOH^+} \times m_{H^+}}{m_{Mg^{2+}}} = \frac{(m_{\Sigma Mg} - m_{Mg^{2+}}) \times m_{H^+}}{m_{Mg^{2+}}} \tag{6}$$

Therefore, using the experimentally determined total magnesium and hydrogen ion concentrations, free magnesium concentrations can be determined by solving Eq. (6) for $m_{Mg^{2+}}$. After obtaining $m_{Mg^{2+}}$, equilibrium quotients for Reaction (3) can be computed according to the following equation:

$$Q_{s2} = \frac{m_{Mg^{2+}}}{(m_{H^+})^2} \tag{7}$$

Table 3. Solubilities of brucite in NaCl solutions at elevated temperatures determined in this work

Exp. #	T, C	NaCl, mol•kg^{-1}	Exp. time, d	pH	pH$_m$	m$_{\Sigma Mg}$, mol•kg^{-1}
Brucite-0.01-1 40C	40	0.01	112	9.71	9.71	1.48E-03
			209	9.67	9.67	1.54E-03
			344	9.66	9.66	1.72E-03
Brucite-0.01-2 40C	40	0.01	112	9.75	9.75	1.48E-03
			209	9.69	9.69	1.59E-03
			344	9.65	9.65	1.88E-03
Brucite-0.1-1 40C	40	0.1	112	9.81	9.81	1.69E-03
			211	9.81	9.81	1.67E-03
			344	9.76	9.76	1.90E-03
Brucite-0.1-2 40C	40	0.1	112	9.82	9.82	1.76E-03
			211	9.85	9.85	1.70E-03
			344	9.76	9.79	1.89E-03
Brucite-1.0-1 40C	40	1.0	112	9.82	9.82	2.47E-03
			211	9.70	9.70	2.99E-03
			344	9.74	9.74	3.37E-03
Brucite-1.0-2 40C	40	1.0	112	9.78	9.78	2.35E-03
			211	9.73	9.73	2.39E-03
			344	9.77	9.77	2.65E-03
Brucite-2.0-1 40C	40	2.1	112	9.68	9.85	2.57E-03
			211	9.63	9.80	2.54E-03
			344	9.69	9.86	2.75E-03
Brucite-2.0-2 40C	40	2.1	112	9.67	9.84	2.58E-03
			211	9.64	9.81	2.44E-03
			344	9.68	9.85	2.68E-03
Brucite-3.0-1 40C	40	3.2	112	9.44	9.77	2.61E-03
			211	9.46	9.79	2.61E-03
			344	9.51	9.84	3.22E-03
Brucite-3.0-2 40C	40	3.2	112	9.41	9.74	2.58E-03
			211	9.39	9.72	3.44E-03
			344	9.45	9.78	4.31E-03

Exp. #	**T, C**	**NaCl, mol•kg^{-1}**	**Exp. time, d**	**pH**	**pH$_m$**	**m$_{\Sigma Mg}$, mol•kg^{-1}**
Brucite-4.0-1 40C	40	4.4	112	9.27	9.79	2.45E-03
			211	9.32	9.84	2.91E-03
			344	9.33	9.85	4.12E-03
Brucite-4.0-2 40C	40	4.4	112	9.30	9.82	2.44E-03
			211	9.36	9.88	2.47E-03
			344	9.41	9.93	2.68E-03
Brucite-5.0-1 40C	40	5.6	112	9.18	9.89	2.30E-03
			211	9.19	9.90	2.26E-03
			344	9.25	9.96	2.95E-03
Brucite-5.0-2 40C	40	5.6	112	9.19	9.90	2.30E-03
			211	9.19	9.90	2.51E-03
			344	9.24	9.95	2.79E-03
Brucite-0.01-1 50C	50	0.01	111	9.43	9.43	1.63E-03
			205	9.50	9.50	1.94E-03
			343	9.45	9.45	2.07E-03
Brucite-0.01-2 50C	50	0.01	111	9.51	9.51	1.64E-03
			205	9.45	9.45	1.66E-03
			343	9.49	9.49	1.73E-03
Brucite-0.1-1 50C	50	0.1	111	9.70	9.70	1.84E-03
			205	9.52	9.52	1.95E-03
			343	9.54	9.54	2.17E-03
Brucite-0.1-2 50C	50	0.1	111	9.72	9.72	1.85E-03
			205	9.53	9.53	1.80E-03
			343	9.57	9.57	1.92E-03
Brucite-1.0-1 50C	50	1.0	111	9.50	9.48	2.57E-03
			205	9.50	9.48	2.51E-03
			343	9.56	9.54	2.66E-03
Brucite-1.0-2 50C	50	1.0	111	9.55	9.53	2.62E-03
			205	9.48	9.46	2.61E-03
			343	9.57	9.55	2.78E-03
Brucite-2.0-1 50C	50	2.1	111	9.26	9.47	2.84E-03
			205	9.37	9.59	2.81E-03
			343	9.42	9.64	3.03E-03

Table 3. (Continued)

Exp. #	T, C	NaCl, mol•kg^{-1}	Exp. time, d	pH	pH$_m$	m$_{\Sigma Mg}$, mol•kg^{-1}
Brucite-2.0-2 50C	50	2.1	111	9.39	9.60	2.66E-03
			205	9.38	9.59	2.74E-03
			343	9.49	9.70	2.79E-03
Brucite-3.0-1 50C	50	3.2	112	9.07	9.41	2.80E-03
			205	9.26	9.60	2.58E-03
			343	9.35	9.69	2.79E-03
Brucite-3.0-2 50C	50	3.2	112	8.98	9.32	2.67E-03
			205	9.23	9.57	2.59E-03
			343	9.36	9.70	2.69E-03
Brucite-4.0-1 50C	50	4.4	112	9.01	9.54	2.58E-03
			205	9.10	9.63	2.44E-03
			343	9.11	9.64	2.59E-03
Brucite-4.0-2 50C	50	4.4	112	8.98	9.51	2.72E-03
			205	9.08	9.61	2.49E-03
			343	9.18	9.71	3.04E-03
Brucite-5.0-1 50C	50	5.6	112	8.89	9.58	2.40E-03
			205	8.97	9.66	2.27E-03
			343	9.09	9.78	2.49E-03
Brucite-5.0-2 50C	50	5.6	112	8.89	9.58	2.45E-03
			205	8.97	9.66	2.35E-03
			343	9.09	9.78	2.51E-03
Brucite-0.01-1 60C	60	0.01	105	9.22	9.22	1.60E-03
			127	9.30	9.30	1.61E-03
			342	9.22	9.22	2.09E-03
Brucite-0.01-2 60C	60	0.01	105	9.23	9.23	1.65E-03
			127	9.31	9.31	1.61E-03
			342	9.32	9.32	1.80E-03
Brucite-0.1-1 60C	60	0.1	105	9.34	9.34	2.00E-03
			127	9.25	9.25	1.97E-03
			342	9.33	9.54	2.21E-03

Exp. #	**T, C**	**NaCl, mol•kg^{-1}**	**Exp. time, d**	**pH**	**pH$_m$**	**m$_{\Sigma Mg}$, mol•kg^{-1}**
Brucite-0.1-2 60C	60	0.1	105	9.30	9.30	1.87E-03
			127	9.27	9.27	1.85E-03
			342	9.33	9.33	1.97E-03
Brucite-1.0-1 60C	60	1.0	105	9.26	9.32	2.48E-03
			127	9.27	9.33	2.47E-03
			342	9.37	9.43	2.63E-03
Brucite-1.0-2 60C	60	1.0	105	9.23	9.29	2.56E-03
			127	9.28	9.34	2.47E-03
			342	9.37	9.43	2.65E-03
Brucite-2.0-1 60C	60	2.1	105	9.13	9.32	2.72E-03
			127	9.18	9.37	2.64E-03
			342	9.27	9.46	2.75E-03
Brucite-2.0-2 60C	60	2.1	105	9.12	9.31	2.67E-03
			127	9.17	9.36	2.57E-03
			342	9.27	9.46	2.84E-03
Brucite-3.0-1 60C	60	3.2	105	9.03	9.43	2.72E-03
			127	9.09	9.49	2.68E-03
			342	9.14	9.54	3.01E-03
Brucite-3.0-2 60C	60	3.2	105	9.02	9.43	2.72E-03
			127	9.09	9.49	2.69E-03
			342	9.11	9.51	2.85E-03
Brucite-4.0-1 60C	60	4.4	105	8.93	9.52	2.70E-03
			127	9.01	9.60	2.53E-03
			342	9.06	9.65	2.82E-03
Brucite-4.0-2 60C	60	4.4	105	8.86	9.45	2.63E-03
			127	8.99	9.58	2.56E-03
			342	9.07	9.66	2.64E-03
Brucite-5.0-1 60C	60	5.6	105	8.78	9.48	2.44E-03
			127	8.85	9.55	2.39E-03
			342	8.95	9.65	2.60E-03
Brucite-5.0-2 60C	60	5.6	105	8.80	9.50	2.36E-03
			127	8.86	9.56	2.39E-03
			342	8.95	9.65	2.47E-03

Table 3. (Continued)

Exp. #	T, C	NaCl, mol•kg^{-1}	Exp. time, d	pH	pH_m	$m_{\Sigma Mg}$, mol•kg^{-1}
Brucite-0.01-1 70C	70	0.01	104	8.97	8.97	1.68E-03
			126	9.02	9.02	1.72E-03
			342	9.02	9.02	1.84E-03
Brucite-0.01-2 70C	70	0.01	104	8.95	8.95	1.65E-03
			126	9.04	9.04	1.64E-03
			342	9.02	9.02	1.71E-03
Brucite-0.1-1 70C	70	0.1	104	9.00	9.00	1.87E-03
			126	9.08	9.08	1.83E-03
			342	9.06	9.06	2.00E-03
Brucite-0.1-2 70C	70	0.1	104	9.07	9.07	2.15E-03
			126	9.09	9.09	1.94E-03
			342	9.07	9.07	2.09E-03
Brucite-1.0-1 70C	70	1.0	104	8.95	9.05	2.58E-03
			126	9.01	9.11	2.45E-03
			342	9.04	9.14	2.76E-03
Brucite-1.0-2 70C	70	1.0	104	8.93	9.03	2.60E-03
			126	9.05	9.15	2.56E-03
			342	9.03	9.13	2.71E-03
Brucite-2.0-1 70C	70	2.1	104	8.83	9.04	2.64E-03
			126	8.98	9.19	2.54E-03
			342	8.98	9.19	2.80E-03
Brucite-2.0-2 70C	70	2.1	104	8.86	9.07	2.67E-03
			126	8.98	9.19	2.57E-03
			342	8.98	9.19	2.87E-03
Brucite-3.0-1 70C	70	3.2	104	8.74	9.13	2.60E-03
			126	8.89	9.28	2.64E-03
			342	8.82	9.21	2.73E-03
Brucite-3.0-2 70C	70	3.2	104	8.74	9.13	2.62E-03
			126	8.89	9.28	2.70E-03
			342	8.82	9.21	2.62E-03

Exp. #	**T, C**	**NaCl, mol•kg^{-1}**	**Exp. time, d**	**pH**	**pH$_m$**	**m$_{\Sigma Mg}$, mol•kg^{-1}**
Brucite-4.0-1 70C	70	4.4	104	8.63	9.18	2.47E-03
			126	8.85	9.40	2.43E-03
			342	8.76	9.31	2.67E-03
Brucite-4.0-2 70C	70	4.4	104	8.63	9.18	2.49E-03
			126	8.84	9.39	2.57E-03
			342	8.77	9.32	2.60E-03
Brucite-5.0-1 70C	70	5.6	104	8.63	9.34	2.38E-03
			126	8.76	9.47	2.33E-03
			342	8.65	9.38	2.54E-03
Brucite-5.0-2 70C	70	5.6	104	8.59	9.30	2.50E-03
			126	8.72	9.43	2.51E-03
			342	8.64	9.35	2.44E-03
Brucite-0.01-1 80C	80	0.01	72	8.84	8.84	1.51E-03
			120	8.84	8.84	1.58E-03
Brucite-0.01-2 80C	80	0.01	72	8.85	8.85	1.60E-03
			120	8.92	9.02	1.74E-03
Brucite-0.1-1 80C	80	0.1	72	8.89	8.89	1.79E-03
			120	8.81	8.81	1.93E-03
Brucite-0.1-2 80C	80	0.1	72	8.88	8.88	1.76E-03
			120	8.98	8.98	2.02E-03
Brucite-1.0-1 80C	80	1.0	72	8.80	8.90	2.30E-03
			120	8.84	8.94	2.81E-03
Brucite-1.0-2 80C	80	1.0	72	8.79	8.89	2.32E-03
			120	8.90	9.00	2.64E-03
Brucite-2.0-1 80C	80	2.1	72	8.85	9.07	2.57E-03
			120	8.84	9.06	2.93E-03
Brucite-2.0-2 80C	80	2.1	72	8.86	9.08	2.61E-03
			120	8.83	9.05	3.26E-03
Brucite-3.0-1 80C	80	3.2	72	8.72	9.14	2.37E-03
			120	8.70	9.12	2.61E-03
Brucite-3.0-2 80C	80	3.2	72	8.71	9.13	2.40E-03
			120	8.79	9.21	2.75E-03
Brucite-4.0-1 80C	80	4.4	72	8.60	9.16	2.32E-03
			120	8.69	9.25	2.78E-03

Table 3. (Continued)

Exp. #	T, C	NaCl, mol•kg^{-1}	Exp. time, d	pH	pH$_m$	m$_{\Sigma Mg}$, mol•kg^{-1}
Brucite-4.0-2 80C	80	4.4	72	8.61	9.17	2.32E-03
			120	8.71	9.27	2.63E-03
Brucite-5.0-1 80C	80	5.6	72	8.52	9.17	2.15E-03
			120	8.65	9.30	2.41E-03
Brucite-5.0-2 80C	80	5.6	72	8.50	9.17	2.13E-03
			120	8.64	9.29	2.46E-03

The equilibrium quotients for Reaction (3) determined in this study are tabulated in Table 4.

Table 4. Equilibrium quotients for Reaction (3) determined in this study

T, ºC	m$_{NaCl}$, mol•kg^{-1}	log Q_{s2}, ± 2σ
40	0.010	16.57 ± 0.09
	0.10	16.85 ± 0.09
	1.0	16.92 ± 0.15
	2.1	17.07 ± 0.13
	3.2	17.03 ± 0.25
	4.4	17.15 ± 0.27
	5.6	17.23 ± 0.22
50	0.010	16.17 ± 0.16
	0.10	16.46 ± 0.33
	1.0	16.42 ± 0.17
	2.1	16.63 ± 0.30
	3.2	16.51 ± 0.61
	4.4	16.64 ± 0.32
	5.6	16.74 ± 0.38
60	0.010	15.74 ± 0.18
	0.10	15.88 ± 0.18
	1.0	16.11 ± 0.25

T, °C	m_{NaCl}, mol•kg^{-1}	log $Q_{s2,} \pm 2\sigma$
	2.1	16.17 ± 0.27
	3.2	16.37 ± 0.21
	4.4	16.56 ± 0.32
	5.6	16.51 ± 0.31
70	0.010	15.21 ± 0.15
	0.10	15.39 ± 0.15
	1.0	15.60 ± 0.20
	2.1	15.70 ± 0.28
	3.2	15.81 ± 0.27
	4.4	15.97 ± 0.38
	5.6	16.13 ± 0.24
80	0.010	14.89 ± 0.20
	0.10	15.02 ± 0.29
	1.0	15.24 ± 0.26
	2.1	15.54 ± 0.06
	3.2	15.64 ± 0.20
	4.4	15.79 ± 0.29
	5.6	15.79 ± 0.37

Using the SIT coefficients, ε(Mg^{2+}, Cl^-) and ε(H^+, Cl^-), from Xiong (2006), at the experimental temperatures for this work, the equilibrium quotients in Table 4 are extrapolated to infinite dilution based on the following equation,

$$\log_{10} K^0_{s2} = \log_{10} Q_{s2} - 2D + \varepsilon(Mg^{2+}, Cl^-) I_m - 2\varepsilon(H^+, Cl^-) I_m + 2\log_{10} a_{H_2O} \quad (8)$$

where $\log K^0_{s2}$ is an equilibrium constant at infinite dilution for Reaction (3); $\log Q_{s2}$ an equilibrium quotient for Reaction (3) at certain ionic strengths; *D* the Debye-Hückel term defined by the following equation; I_m ionic strength on a molal scale; a_{H_2O} activity of water,

$$D = \frac{A_\gamma \sqrt{I_m}}{1+1.5\times\sqrt{I_m}} \tag{9}$$

where A_γ is Debye-Hückel slope for activity coefficients.

In using Equations (8) and (9) to extrapolate to infinite dilution, the activities of water in NaCl solutions under the experimental conditions are from Gibbard et al., (1974), and the Debye-Hückel slopes for activity coefficients at the experimental temperatures of this work are from Helgeson et al., (1981). The equilibrium constants for Reaction (3) at infinite dilution are listed in Table 5.

In Figure 4, the solubility constants at infinite dilution as a function of reciprocal temperature are displayed. In this figure, the $\log_{10} K_{s2}^0$ at 25°C from Xiong (2008) is also included. The temperature function of $\log_{10} K_{s2}^0$ can be described by the following expression:

$$\log_{10} K_{s2}^0 = \frac{4306.8369}{T} + 2.6383 \tag{10}$$

where *T* is temperature in K. In the linear regression, the $\log_{10} K_{s2}^0$ at 25°C from Xiong (2008) is also incorporated.

Table 5. Equilibrium constants for Reaction (3) at infinite dilution determined in this work

Temperature, °C	$\log_{10} K_{s2}^0 \pm 2\sigma$
40	16.43 ± 0.22
50	15.96 ± 0.32
60	15.63 ± 0.11
70	15.12 ± 0.08
80	14.84 ± 0.16

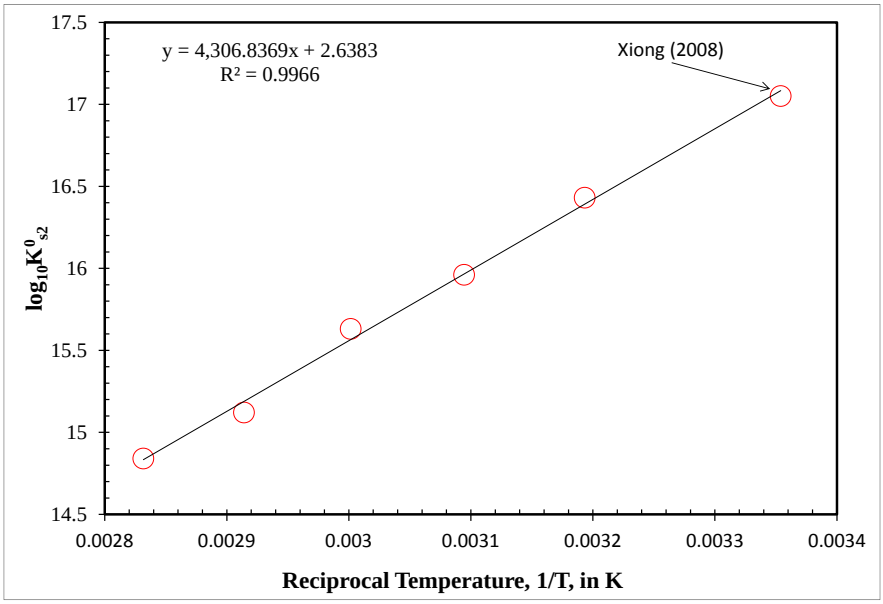

Figure 4. A plot showing the solubility constants at infinite dilution as a function of reciprocal temperature. Notice that the data point at 25ºC from Xiong (2008) is also included in the regression.

CONCLUSION

In this study, we have determined the solubility constants of brucite in NaCl solution at elevated temperatures up to 80ºC. The hydrogen ion concentrations in our experiments in NaCl solutions to high ionic strength at elevated temperatures are determined by applying the correction factors that are experimentally acquired in this work. As brines associated with salt formations are of high ionic strength in nature, the results from our work are applicable to nuclear waste isolation in salt formations. They are also relevant for modeling the formation of brucite-carbonate chimneys in hyperalkaline (pH 9-11), saline, hydrothermal fluids (40ºC to 90ºC). Based on the highly linear relation between the solubility constant of brucite and temperature, the solubility constants of brucite can be accurately extrapolated down to 0ºC, and up to 100ºC.

ACKNOWLEDGMENTS

Sandia National Laboratories is a multi-mission laboratory managed and operated by National Technology and Engineering Solutions of Sandia, L.L.C., a wholly owned subsidiary of Honeywell International, Inc., for the U.S. Department of Energy's National Nuclear Security Administration under contract DE-NA-0003525. This research is funded by the Salt R&D programs administered by the Office of Nuclear Energy (NE) of the U.S. Department of Energy.

REFERENCES

Altmaier, M., V. Metz, V. Neck, R. Müller, and Th Fanghänel, 2003. "Solid-liquid equilibria of $Mg(OH)_2$(cr) and $Mg_2(OH)_3Cl{\bullet}4H_2O$(cr) in the system Mg-Na-H-OH-Cl-H_2O at 25ºC." *Geochimica et Cosmochimica Acta* 67, 3595–3601.

Behlau, J. and Mingerzahn, G., 2001. "Geological and tectonic investigations in the former Morsleben salt mine (Germany) as a basis for the safety assessment of a radioactive waste repository." *Engineering Geology* 61, 83–97.

Brewitz, W., Droste, J. and Stier-Friedland, G., 2008. "Geological features of the Morsleben repository and their relevance for long-term safety." *Reviews in Engineering Geology* 19, 53-66.

Gibbard Jr, H. Frank, George Scatchard, Raymond A. Rousseau, and Jefferson L. Creek, 1974. "Liquid-vapor equilibrium of aqueous sodium chloride, from 298 to 373. deg. K and from 1 to 6 mol kg^{-1}, and related properties." *Journal of Chemical and Engineering Data* 19, 281–288.

Helgeson, Harold C., David H. Kirkham, and George C. Flowers, 1981. "Theoretical prediction of the thermodynamic behavior of aqueous electrolytes by high pressures and temperatures; IV, Calculation of activity coefficients, osmotic coefficients, and apparent molal and

standard and relative partial molal properties to 600 degrees C and 5kb." *American Journal of Science* 281, 1249–1516.

Krumhansl, J. L., Panenguth, H. W., Zhang, P. C., Kelly, J. W., Anderson, H. L., Hardesty, J. O., 2000. "Behavior of MgO as a CO_2 scavenger at the Waste Isolation Pilot Plant (WIPP), Carlsbad, New Mexico." *Materials Research Society Symposium Proceedings* 608, 155–160.

Monnin, C., V. Chavagnac, C. Boulart, B. Ménez, Martine Gérard, E. Gérard, C. Pisapia, M. Quemeneur, G. Erauso, A. Postec, and L. Guentas-Dombrowski, 2014. "Fluid chemistry of the low temperature hyperalkaline hydrothermal system of Prony Bay (New Caledonia)." *Biogeosciences* 11, no. 20, 5687.

Okumura, T., Y. Ohara, R. J. Stern, T. Yamanaka, Y. Onishi, H. Watanabe, C. Chen, S. H. Bloomer, I. Pujana, S. Sakai, T. Ishii, 2016. "Brucite chimney formation and carbonate alteration at the Shinkai Seep Field, a serpentinite-hosted vent system in the southern Mariana forearc." *Geochemistry, Geophysics, Geosystems* 17, 3775–3796.

Palmer, Donald A., and David J. Wesolowski, 1997. "Potentiometric measurements of the first hydrolysis quotient of magnesium (II) to 250 C and 5 molal ionic strength (NaCl)." *Journal of Solution Chemistry* 26, 217–232.

Schuessler, W., B. Kienzler, S. Wilhelm, V. Neck, and J. I. Kim, 2001. "Modeling of Near Field Actinide Concentrations in Radioactive Waste Repositories in Salt Formations: Effect of Buffer Materials." *Mat. Res. Soc. Symp. Proc.* 663, 791.

Schwartz, M. O., 2012. Modelling groundwater contamination above a nuclear waste repository at Gorleben, Germany. *Hydrogeology Journal* 20, 533-546.

Sőhnel, O, Novotný, P., 1985. *Densities of aqueous solutions of inorganic substances*. Elsevier, New York, 335 p.

Stewart, S., 2002. Exploring the continental shelf for low geological risk nuclear waste repository sites using petroleum industry databases: a UK case study. *Engineering Geology* 67, 139-168.

U.S. National Academy of Sciences Committee on Waste Disposal. 1957. *The Disposal of Radioactive Waste on Land*. Publication 519.

Washington, DC: National Academy of Sciences–National Research Council.

Wood, S. A., Palmer, D. A., Wesolowski, D. J., Bénézeth, P., 2002. "The aqueous geochemistry of the rare earth elements and yttrium. Part XI. The solubility of $Nd(OH)_3$ and hydrolysis of Nd^{3+} from 30 to 290°C at saturated water vapor pressure with in-situ pHm measurement." In: Hellmann, R. and Wood, S. A., (Eds.), *Water-Rock Interactions, Ore Deposits, and Environmental Geochemistry: A Tribute to David Crerar*, Special Publication 7, The Geochemical Society, pp. 229–256.

Xiong, Y. L., 2003. "Revised thermodynamic properties of brucite determined by solubility studies and its significance to nuclear waste isolation." In *Abstracts with Programs, Geological Society of America Annual Meeting (Seattle, Washington*, vol. 35, no. 6, pp. 102-103.

Xiong, Y. L., 2006. "Estimation of medium effects on equilibrium constants in moderate and high ionic strength solutions at elevated temperatures by using specific interaction theory (SIT): interaction coefficients involving Cl^-, OH^- and Ac^- up to 200°C and 400 bars." *Geochemical Transactions* 7, no. 1: 4.

Xiong, Yongliang, 2008. "Thermodynamic properties of brucite determined by solubility studies and their significance to nuclear waste isolation." *Aquatic Geochemistry* 14, 223–238.

Xiong, Y. L., and A. C. S. Lord, 2008. "Experimental investigations of the reaction path in the $MgO–CO_2–H_2O$ system in solutions with ionic strengths, and their applications to nuclear waste isolation." *Applied Geochemistry* 23, 1634–1659.

Xiong, Y. L., H. Deng, M. Nemer, S. Johnsen, 2010. "Experimental determination of the solubility constant for magnesium chloride hydroxide hydrate ($Mg_3Cl(OH)_5•4H_2O$, phase 5) at room temperature, and its importance to nuclear waste isolation in geological repositories in salt formations." *Geochimica et Cosmochimica Acta* 74, 4605–4611.